

The temperature dependent anisotropy constants of epitaxially grown PrCo_{5+x}

A. K. Patra,^{1,2,a)} M. Eisterer,³ R. Biele,² S. Fähler,^{1,2} L. Schultz,^{1,2} and V. Neu^{1,2,b)}

¹*Institute for Metallic Materials, IFW Dresden, P.O. Box 270116, 01171 Dresden, Germany*

²*Department of Physics, Institute for Solid State Physics, Dresden University of Technology, 01062 Dresden, Germany*

³*Atomic Institute of the Austrian Universities Vienna, Stadionallee 2, 1020 Vienna, Austria*

(Received 13 July 2010; accepted 16 August 2010; published online 5 October 2010)

The temperature dependent anisotropy of a highly textured epitaxial Pr–Co film with a single orientation of the crystallographic *c*-axis along MgO[001] is investigated by measuring angle dependent hysteresis loops at various temperatures. The measured magnetization curves are compared with calculated magnetization curves, which allows for a full analysis of the temperature dependent anisotropy constants of first and second order, K_1 and K_2 and the determination of the saturation polarization. The analysis reveals that the $\text{Pr}_{15.4}\text{Co}_{84.6}$ film undergoes a spin reorientation transition from an easy axis anisotropy to an easy cone anisotropy at 108 K. The room temperature values of K_1 and K_2 measured for this $\text{Pr}_{15.4}\text{Co}_{84.6}$ film are 5.0 MJ m^{-3} and 0.5 MJ m^{-3} , respectively. The difference to the bulk PrCo_5 single crystal values is ascribed to the high Co content of the $\text{Pr}_{15.4}\text{Co}_{84.6}$ film. © 2010 American Institute of Physics. [doi:10.1063/1.3490204]

I. INTRODUCTION

RECo_5 (RE=rare earth) compounds are of both fundamental and technological interest, due to their excellent intrinsic magnetic properties such as a high Curie temperature T_C , a high saturation polarization J_S , and a complex and often temperature dependent magnetocrystalline anisotropy (MCA). RECo_5 compounds crystallize in a hexagonal CaCu_5 structure ($P6/mmm$) (Co occupies $2c$ and $3g$ sites and RE takes $1a$ site).^{1,2} The simple crystal structure of the RECo_5 phase and the existence of isostructural compounds with different RE or transition metal species make the RECo_5 compounds a suitable model system to investigate the atomistic origin of MCA and its effects on the magnetic properties.

So far as PrCo_5 is concerned, it meets the requirements to qualify for a permanent magnet material and possesses the highest theoretical energy product within the RECo_5 series. Furthermore, PrCo_5 exhibits a spin reorientation (SR) transition from an easy axis anisotropy along the crystallographic *c*-axis (which persists above the transition temperature) to an easy cone anisotropy around 107 K.³

In our earlier report,⁴ we revealed that epitaxial Pr–Co films ($\approx 80 \text{ nm}$) can be prepared on Cr buffered MgO(110) substrates in a wide composition range with a single orientation of the *c*-axis which lies in the film plane along the MgO[001] substrate edge. In that series, Pr–Co films crystallize in different phases like the PrCo_7 structure^{5,6} and the PrCo_5 and Pr_2Co_7 phases, which exist in a certain composition range. These highly textured epitaxial Pr–Co films exhibit excellent intrinsic and extrinsic magnetic properties. Pr–Co films in the composition range of $15.4 \leq \text{Pr at. \%} \leq 20.4$ crystallize in a mixed phase of the hard magnetic hexagonal PrCo_5 and Pr_2Co_7 phases and possess an energy

density value of up to $(BH)_{\text{max}}=310 \text{ kJ/m}^3$ at room temperature. However, this energy density value measured for a $\text{Pr}_{15.4}\text{Co}_{84.6}$ film, with a room temperature saturation polarization $J_S=1.4 \text{ T}$, is below the theoretical energy density value of $(BH)_{\text{max}}^{\text{th}}=J_S^2/4\mu_0=390 \text{ kJ/m}^3$, which holds for $J_R=J_S$ and $\mu_0H_C>1/2J_S$ (Ref. 7). In this Pr–Co film with its coercivity of $\mu_0H_C=0.66 \text{ T}$, the condition of $\mu_0H_C>1/2J_S$ is not satisfied and therefore raises the question concerning the limits in coercivity and possible improvements. For both, the upper theoretical limit of coercivity and the detailed coercivity mechanism a precise knowledge of the MCA as the main origin of coercivity has to be known. Furthermore, to test coercivity models such as coherent rotation, nucleation, and domain wall pinning, a good set of temperature dependent data for the saturation polarization and the anisotropy constants K_1 and K_2 is needed.⁸

In this paper, we carefully examine the MCA, including the SR, in an epitaxial $\text{Pr}_{15.4}\text{Co}_{84.6}$ film with an energy density of 310 kJ/m^3 and determine the temperature dependency of the anisotropy constants and saturation polarization. To this end, magnetization measurements are carried out at various temperatures with the field applied at different angles with respect to the texture axis of the sample and are compared with the calculated magnetization curves. The full set of $K_1(T)$, $K_2(T)$, and $J_S(T)$ data for this thin film sample is discussed with respect to values found in single crystals and with respect to the measured coercivity.

II. EXPERIMENTAL

Epitaxial Pr–Co films ($\approx 80 \text{ nm}$) with $(1\bar{1}00)$ orientation (having *c*-axis in the film plane only along MgO[001] substrate edge) were grown on heated Cr buffered MgO(110) substrates using pulsed laser deposition from metallic targets.⁴

^{a)}Electronic mail: ajit.patra@uni-konstanz.de.

^{b)}Electronic mail: v.neu@ifw-dresden.de.

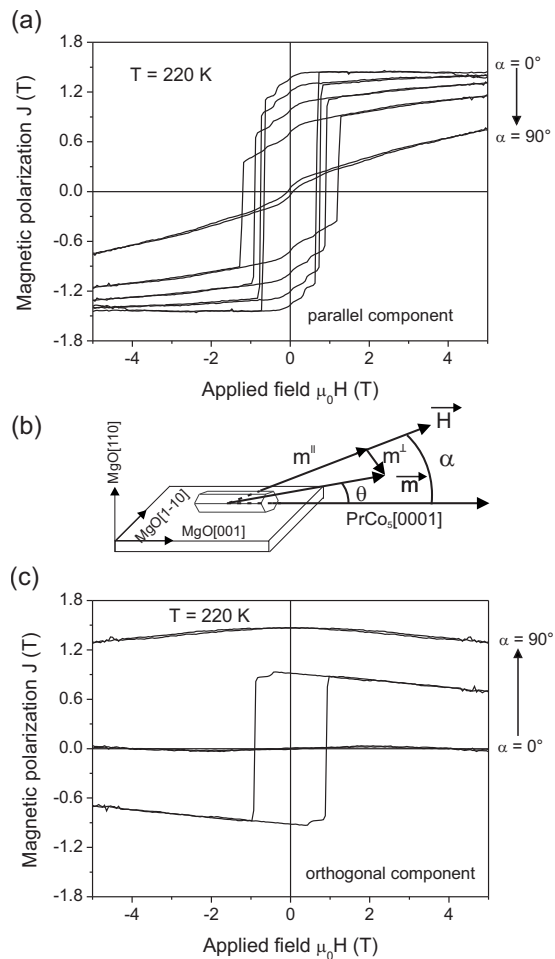


FIG. 1. Hysteresis loops of the epitaxial $\text{Pr}_{15.4}\text{Co}_{84.6}$ film measured at 220 K for different angles α between the applied field and the texture axis: (a) parallel component of the magnetic polarization vector for $\alpha=0^\circ, 30^\circ, 45^\circ, 60^\circ,$ and 90° , (b) schematic sketch showing the field direction with respect to the sample orientation, and (c) orthogonal component of the magnetic polarization vector for $\alpha=0^\circ, 45^\circ,$ and 90° . θ is the angle between the texture axis and the magnetic polarization vector.

In order to investigate the temperature dependent anisotropy of an epitaxial $\text{Pr}_{15.4}\text{Co}_{84.6}$ film, angle dependent magnetization measurements with magnetic field applied along different angles α [sketch Fig. 1(b)] with respect to the texture axis (crystallographic c -axis) have been carried out at various temperatures. Measurements are performed in a split coil vibrating-sample magnetometer with a maximum field of 5 T in a temperature range between 5 and 300 K. The experimental facility allows to measure simultaneously both, the parallel and the orthogonal components of the magnetization for a given field and therefore the total (saturated) magnetization could be evaluate experimentally. From the measurement of only the parallel component of the magnetization vector it is not possible to derive the saturation magnetization of compounds, if the applied field is not large enough to saturate the sample, and it is not straightforward for compounds exhibiting SR transition. In the available experimental setup, we have access only to two (both in-plane) components of the magnetization vector. For the present case of a sample with easy axis and applied field always in the film plane, the magnetization distribution inside the sample

will also be confined largely to the film plane (supported by the shape anisotropy). Thus, the additional measurement of the transversal component throughout the hysteresis allows the reconstruction of the total magnetization vector.

The measurements are carried out on a $5\text{ mm} \times 5\text{ mm}$ epitaxial $\text{Pr}_{15.4}\text{Co}_{84.6}$ film with the angle α varying from $\alpha=0^\circ$ (parallel to c -axis: along $\text{MgO}[001]$) to $\alpha=90^\circ$ (parallel to in-plane hard axis: along $\text{MgO}[1\bar{1}0]$) [Fig. 1(b)]. The sample is first saturated along the c -axis (easy axis at room temperature) at the highest available positive field of 5 T, then the reversed field is applied and the corresponding magnetization curves are recorded. Before starting the measurement for a new angle α , the sample was always saturated along the c -axis at 5 T to ensure a similar initial state for every measurement. To determine the anisotropy constants a full range fitting procedure to the magnetization loops in a field range of 2–5 T is performed. The theoretical magnetization loops were calculated based on an energy minimization code including anisotropy energy developed up to second order (K_1 and K_2) and magnetostatic energy of the magnetization vector in an applied field. A realistic texture spread of 10° was implemented by averaging over a Gauss shaped c -axis distribution around the texture axis of the sample. For a given temperature, measurements at five different angles were fitted simultaneously to derive the first and second order anisotropy constants (K_1 and K_2).

III. RESULTS AND DISCUSSION

Shown in Fig. 1 are the background corrected hysteresis loops of the parallel and orthogonal component of the magnetic polarization vector \vec{J} measured at 220 K with the field applied along different angles ($\alpha=0^\circ, 30^\circ, 45^\circ, 60^\circ,$ and 90° for parallel component and $\alpha=0^\circ, 45^\circ,$ and 90° for orthogonal component). The field orientation with respect to the grain orientation is shown in the sketch [Fig. 1(b)]. When the field is applied along the c -axis ($\alpha=0^\circ$) a nearly rectangular hysteresis loop is observed for the parallel component $m^{\parallel} = \cos(\alpha - \theta)$ of magnetization [see Fig. 1(a)], as expected for an easy axis measurement (in which case only switching processes occur) of a uniaxial magnet. Here, $\vec{m} = \vec{J}/J_S$ is the normalized magnetization vector and θ is the angle between the texture axis and the vector \vec{m} . As shown in Fig. 1(a), the remanent polarization measured along the c -axis reaches 95% of the saturation polarization (magnetization measured at 5 T in this case) indicating a high degree of alignment of the grains along the c -axis. When the field is applied at an angle to the c -axis (which is the easy axis at this temperature of $T=220\text{ K}$) both switching and rotational processes occur. For higher angles α rotational processes dominate and for $\alpha=90^\circ$ (hard axis case) the magnetization process is purely rotational. Therefore, the magnetization curve measured along the hard axis of a uniaxial magnet is largely nonhysteretic with a linear increase in magnetization with the applied field [Fig. 1(a) $\alpha=90^\circ$ curve]. Furthermore, for the field applied at an angle to the c -axis ($0^\circ < \alpha \leq 90^\circ$), a progressive decrease in the magnetization with increasing angle α is observed. In the remanent state, the magnetic polarization vector (\vec{J}) is parallel to the easy axis. As we are measuring the

component of \vec{J} parallel to the former field axis, this projection decreases with larger α and the remanent polarization as a function of field follows a $\cos \alpha$ dependency. On the other hand, if a positive field is applied, irrespective of α the magnetization will approach the saturation polarization (at least at the anisotropy field) and thus magnetization curves measured at a large angle α will have a large slope as they start from a lower remanent polarization. Both trends (decrease in the remanent polarization and the increase in the slope of the magnetization curves with increase of the angle α) are clearly visible in the measured hysteresis loops [Fig. 1(a)].

In highly textured samples (which is valid in this case), the hysteresis loop measured for the orthogonal component of the magnetization vector [$m^\perp = \sin(\alpha - \theta)$] with field applied along the easy axis ($\alpha = 0^\circ$: c-axis of the sample for PrCo_5) of a uniaxial magnet should exhibit a flat curve parallel to the field axis with negligible value of magnetization. Indeed the measured curve [Fig. 1(c) $\alpha = 0^\circ$] exhibits the expected behavior. When the field is applied along the hard axis ($\alpha = 90^\circ$), the orthogonal component of the magnetization vector [$m^\perp = \cos(\theta)$] should follow the $\cos \theta$ (where θ is the angle between the easy axis and the vector \vec{m}) dependency as a function of applied field, and should have a closed loop (because the magnetization process is purely rotational), which is clearly observed in the measurement [see Fig. 1(c)]. Moreover, for the field applied at angles between the easy axis and hard axis ($0^\circ < \alpha < 90^\circ$) the magnetization loops measured for the orthogonal component exhibit hysteric behavior in which both the switching and rotational processes come into play. An example of a magnetization loop measured for the orthogonal component of the magnetic polarization vector with field applied at an angle of 45° to the c-axis is shown in Fig. 1(c).

A behavior similar to that described in Fig. 1(a) but with slightly higher overall values of the magnetization is observed for magnetization loops measured at 150 K (not shown here). The increased magnetization arises from the temperature dependency of the saturation polarization of the $\text{Pr}_{15.4}\text{Co}_{84.6}$ film. This trend continues until the SR occurs at a certain temperature. At the SR transition temperature (T_{SR}), the system undergoes a transition from an easy axis anisotropy, which persists above the transition temperature, to an easy cone anisotropy and the easy magnetization directions make some angle with the c-axis (former easy magnetization direction) by the opening of a cone around the c-axis. Below T_{SR} , the remanence polarization measured for $\alpha = 0^\circ$ has a smaller value than the saturation polarization J_S , which is understood from the projection of the magnetic polarization vector to the field/measurement axis. In this case, the remanence J_R is determined by $\theta = \theta_{\text{SR}}$ and thus: $J_R^\parallel = J_S(\cos \theta_{\text{SR}})$, (where θ_{SR} is the SR angle). Now, if the field is turned on, in order to reduce the Zeeman energy the angle becomes smaller and the magnetization component parallel to the field axis becomes larger. Therefore, the magnetization curve which should be flat above T_{SR} will now be slightly bent upward. It is, however, difficult to observe this small effect in the measured data at 100 K [Fig. 2(a)]. In the case of magnetization curves measured for $\alpha = 90^\circ$ below T_{SR} , the energy (anisotropy and Zeeman energy) minimum is not ob-

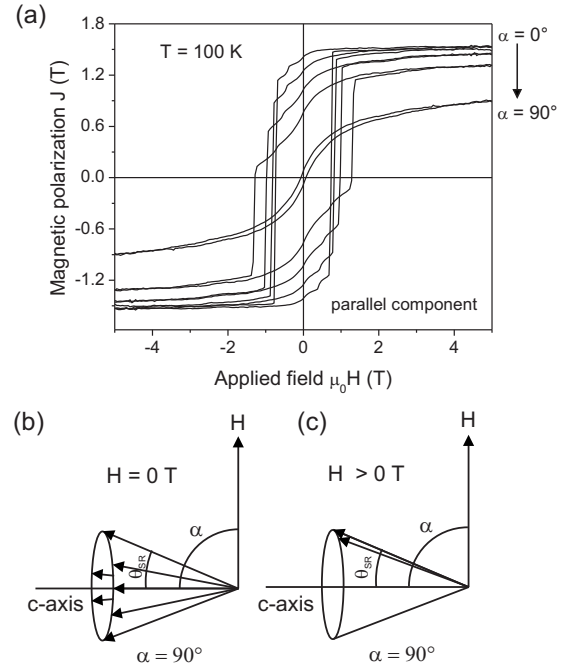


FIG. 2. (a) Hysteresis loops of the epitaxial $\text{Pr}_{15.4}\text{Co}_{84.6}$ film measured at 100 K for various angles α [angles α as in Fig. 1(b)] and [(b) and (c)] schematic picture of the easy magnetization directions below the SR temperature for magnetic field applied perpendicular to the c-axis ($\alpha = 90^\circ$)

served for $\theta = 0^\circ$ but for $\theta = \theta_{\text{SR}}$ [sketch Fig. 2(b)]. However, all the moments lying on the cone will average out and lead to a zero remanent polarization. When the field is applied, a small field value which is sufficient to break the symmetry of the cone will pull all moments toward the field axis and, as a result of this, a sudden increase in the magnetization is expected [sketch Fig. 2(c)]. A further increase in the magnetic field causes the rotation of the moments toward the field axis and a progressive increase in the magnetization for higher fields is expected. Therefore, a reduced slope is expected when approaching saturation polarization and consequently an extrapolation back to zero leads to a nonzero remanence value. As a result of this, the magnetization curves measured at a temperature below T_{SR} for $\alpha = 90^\circ$ are expected to exhibit a S-shape, which is indeed observed for the magnetization curves measured at 100 K. Also the progressive decrease in the magnetization with increasing angle α is still observed below T_{SR} . Similar hysteresis loops are measured for lower temperatures.

In order to evaluate the saturation polarization J_S the vector sum of the parallel and orthogonal components of the magnetic polarization vector for a given field value at a particular angle and temperature is carried out (Fig. 3). This process is repeated for different field values as well as for several field angles and temperatures and from which averaged value of J_S (averaged over all angles) as a function of temperature are constructed. The temperature dependency of J_S obtained from this analysis for the epitaxial $\text{Pr}_{15.4}\text{Co}_{84.6}$ film (open circle) together with the scaled saturation polarization of bulk PrCo_5 (solid line) is plotted in Fig. 3(b). With decreasing temperature J_S increases and follows quite well the expected temperature dependency of the saturation polarization of bulk PrCo_5 .⁹

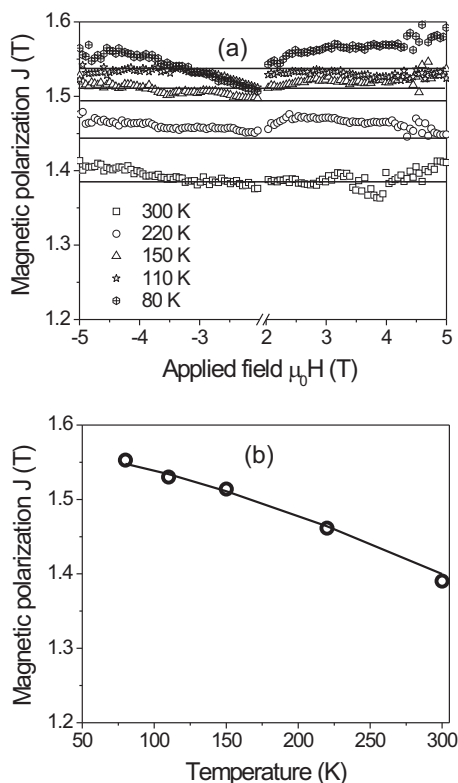


FIG. 3. (a) Vector sum of the parallel and orthogonal components of the polarization vector J of the epitaxial $\text{Pr}_{15.4}\text{Co}_{84.6}$ film results in a constant value as a function of field: the such derived saturation polarization is plotted in (b) as a function of temperature and in comparison with bulk PrCo_5 .

In the following, the evaluation of the anisotropy constants from the measured magnetization curves is considered. To determine the anisotropy constants a full range fitting procedure to the magnetization curves in a field range of 2–5 T (in the first quadrant of the demagnetizing branch) is performed. The theoretical magnetization curves were calculated based on an energy minimization code including anisotropy energy developed up to second order (K_1 and K_2) and magnetostatic energy of the magnetic polarization vector in an applied field.¹⁰ A realistic texture spread of 10° was implemented by averaging over a Gauss shaped c -axis distribution around the texture axis of the sample. For a given temperature, measurements at five different angles were fitted simultaneously to derive the first and second order anisotropy constants K_1 and K_2 . The first quadrant magnetization curves (open circles) of the $\text{Pr}_{15.4}\text{Co}_{84.6}$ film together with the calculated curves (lines) for five different angles at temperatures 300 and 100 K are shown in Fig. 4. The measured curves fit quite well to the calculated curves and the analysis leads to the determination of the first and second order anisotropy constants. Values of $K_1=4.6 \text{ MJ/m}^3$ and $K_2=1.6 \text{ MJ/m}^3$ are obtained at room temperature from this analysis. However, the measured value of $K_1=4.6 \text{ MJ/m}^3$ at room temperature is lower compared to the bulk single crystal value of $K_1=7.7 \text{ MJ/m}^3$ for PrCo_5 (Ref. 3), whereas the value of $K_2=1.6 \text{ MJ/m}^3$ is much higher compared to the value of $K_2=0.05 \text{ MJ/m}^3$ known for bulk PrCo_5 . This difference might be caused by the fact that, in most cases, in order to determine the anisotropy constants of PrCo_5 single

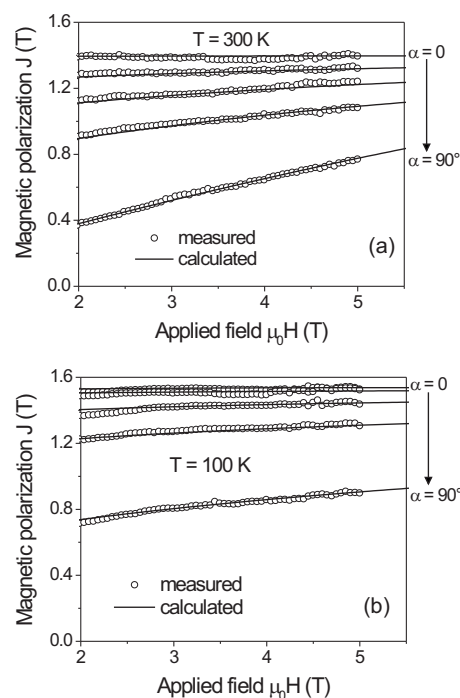


FIG. 4. Measured (open circle) and calculated (line) magnetization curves in the first quadrant for the epitaxial $\text{Pr}_{15.4}\text{Co}_{84.6}$ film at 300 and 100 K [angle α as in Fig. 1(b)].

crystals, the Sucksmith and Thompson approach¹¹ has been used, which only makes use of the hard axis curve to determine the anisotropy constants. Therefore, to effectively compare the anisotropy constant values obtained for the $\text{Pr}_{15.4}\text{Co}_{84.6}$ film with the bulk PrCo_5 single crystal values, only the magnetization curves measured for $\alpha=90^\circ$ have been analyzed, in a similar way to the simultaneous analysis of 5 angles. It turns out that the observed values of $K_1=5.0 \text{ MJ/m}^3$ and $K_2=0.6 \text{ MJ/m}^3$ from the analysis of only the hard axis curve are more close to the values observed for bulk PrCo_5 . The still existing difference is ascribed to the high Co content of the $\text{Pr}_{15.4}\text{Co}_{84.6}$ film, which is optimized for high saturation polarization. It is known that the substitution of Co dumbbells for Co/RE atoms in the RECo_5 structure will lead to a reduced anisotropy, as has been measured, e.g., for YCo_5 and SmCo_5 (Refs. 12 and 13). The different results obtained from the two fitting procedures on the same sample are, however, unexpected and so far its origin is not yet clear. In the subsequent discussion the anisotropy constants obtained from the analysis of the hard axis curve are used. The anisotropy constants K_1 and K_2 as a function of temperature are shown in Fig. 5(a).

The anisotropy constant K_1 decreases with decreasing temperature, changes its sign at $\approx 108 \text{ K}$, and reaches a value of $K_1=-4.8 \text{ MJ/m}^3$ at 20 K. On the other hand, K_2 increases monotonically with decreasing temperature and reaches a value of $K_2=16.1 \text{ MJ/m}^3$ at 20 K. A sign reversal of K_1 at 108 K and K_1, K_2 values which satisfy the condition $2K_2 > -K_1$ (Ref. 14) below 108 K manifest a SR transition from an easy axis to an easy cone anisotropy. The SR angle θ_{SR} (cone angle with respect to the c -axis) which is a function of K_1 and K_2 , varies with temperature according to

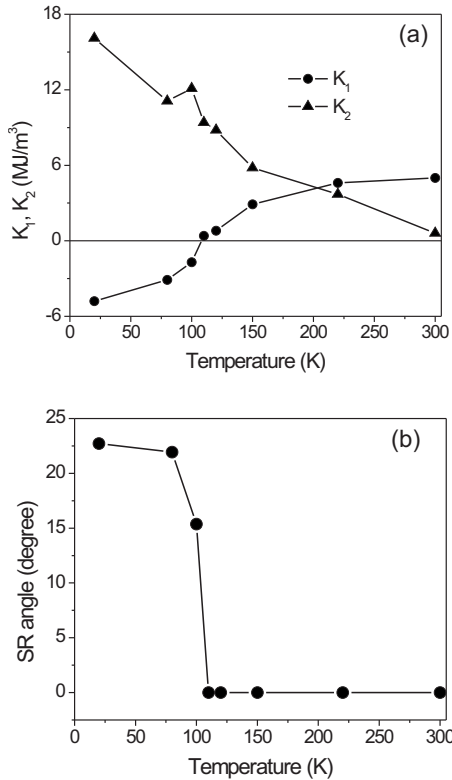


FIG. 5. Temperature dependence of (a) the anisotropy constants K_1 and K_2 and (b) the SR angle of the epitaxial $\text{Pr}_{15.4}\text{Co}_{84.6}$ film.

$$\theta_{\text{SR}} = \arcsin \sqrt{\frac{-K_1}{2K_2}}. \quad (1)$$

In Fig. 5(b), θ_{SR} as a function of temperature is depicted. The critical temperature at which the easy direction of the $\text{Pr}_{15.4}\text{Co}_{84.6}$ film begins to tilt away from the c -axis is 108 K, which is in excellent agreement with the temperature value observed for PrCo_5 single crystals ($T_{\text{SR}}=107$ K (Ref. 3) and $T_{\text{SR}}=102$ K (Ref. 9)). θ_{SR} increases monotonically with decreasing temperature and reaches a value of 22.7° at 20 K. The θ_{SR} value of 22.7° lies in between the value obtained from a direct measurement of the SR angle $\theta_{\text{SR}}=19^\circ$ (Ref. 3) and the value of $\theta_{\text{SR}}=25.7^\circ$ determined from the anisotropy constants for a bulk PrCo_5 single crystal.³ In total, the temperature dependent anisotropy measurement of $\text{Pr}_{15.4}\text{Co}_{84.6}$ film resembles the qualitative behavior (continuous increase in K_2 and decrease in K_1 with decreasing temperature together with a sign reversal of K_1) observed for bulk PrCo_5 . Judging the quantified MCA for its potential in creating highly coercive Pr–Co films, a coercivity analysis, e.g., such as performed on an epitaxial SmCo_5 film,¹⁵ is needed. This is, however, not straightforward in the case of Pr–Co undergoing a SR transition. Therefore the coercivity analysis is beyond the scope of this work. We restrict to a simple estimation based on the coercivity reducing microstructural pa-

rameter $\alpha=0.18$, quantified in an isostructural SmCo_5 film,¹⁵ which was prepared in a comparable manner. This factor predicts a maximum room temperature coercivity of $\mu_0 H_C = \alpha \mu_0 (2K_1/J_S) = 1.6$ T, which is above the observed value. We thus conclude that the MCA of the prepared high moment ($J_S=1.4$ T) $\text{Pr}_{15.4}\text{Co}_{84.6}$ film is sufficient to reach the maximum theoretical energy density, if a microstructure as in the isostructural SmCo_5 film is achieved.

IV. CONCLUSIONS

In summary, angle dependent hysteresis loops measured at various temperatures were carried out to determine temperature dependent saturation polarization, the anisotropy constants and the SR transition of an epitaxial $\text{Pr}_{15.4}\text{Co}_{84.6}$ film with a high energy density. Due to a sign change in K_1 and large increase in K_2 at low temperature this film exhibits a SR transition at $T=108$ K. The values of $K_1 = 5.0$ MJ/m³ and $K_2 = 0.6$ MJ/m³ measured at room temperature for the $\text{Pr}_{15.4}\text{Co}_{84.6}$ film differ from those of bulk PrCo_5 due to the high Co content of the $\text{Pr}_{15.4}\text{Co}_{84.6}$ film. These intrinsic set of data [$K_1(T)$, $K_2(T)$, and $J_S(T)$] are useful for the coercivity analysis, which is essential to boost the coercivity and to improve the energy density of the epitaxial Pr–Co films.

ACKNOWLEDGMENTS

This work is supported by the DFG as part of the SFB 463: “Rare Earth Transition Metal Compounds: Structure, Magnetism, and Transport.”

- ¹J. H. Wernick and S. Geller, *Acta Crystallogr.* **12**, 662 (1959).
- ²K. H. J. Buschow, *Rep. Prog. Phys.* **40**, 1179 (1977).
- ³E. Tatumoto, T. Okamoto, H. Fujii, and C. Inoue, *J. Phys. (Paris)* **32**, C1-550 (1971).
- ⁴A. K. Patra, V. Neu, S. Fähler, R. Groetzschel, S. Bedanta, W. Kleemann, and L. Schultz, *Phys. Rev. B* **75**, 184417 (2007).
- ⁵A. K. Patra, V. Neu, S. Fähler, R. Groetzschel, and L. Schultz, *Appl. Phys. Lett.* **89**, 142512 (2006).
- ⁶A. K. Patra, V. Neu, S. Fähler, and L. Schultz, *J. Phys. D* **40**, 7261 (2007).
- ⁷B. D. Culity, *Introduction to Magnetic Materials* (Addison-Wesley, Reading, MA, 1972).
- ⁸X. C. Kou, H. Kronmüller, D. Govord, and M. F. Rossignol, *Phys. Rev. B* **50**, 3849 (1994).
- ⁹H. P. Klein, A. Menth, and R. S. Perkins, *Physica B & C* **80**, 153 (1975).
- ¹⁰In an applied magnetic field, the total energy density for a hexagonal crystal of CaCu_5 type can be written as $E_{\text{tot}} = K_1 \sin^2 \theta + K_2 \sin^4 \theta - HJ_S \cos(\alpha - \theta)$, where K_1 and K_2 are anisotropy constants, θ is the angle between the crystallographic c -axis and the magnetic polarization vector, H is the magnitude of the external field, J_S is the saturation polarization and α is the angle between the c -axis and applied field direction.
- ¹¹W. Sucksmith and J. E. Thompson, *Proc. R. Soc. London* **67**, 362 (1954).
- ¹²A. V. Korolev, A. S. Yermolenko, A. Y. E. Yermolenko, A. V. Antonov, L. M. Magat, and G. M. Makarova, *Phys. Met. Metallogr.* **39**, 191 (1975).
- ¹³J. Deportes, D. Givord, R. Lemaire, H. Nagai, and Y. T. Yang, *J. Less-Common Met.* **44**, 273 (1976).
- ¹⁴P. A. Algarabel, A. Del Moral, M. R. Ibarra, and J. I. Arnaudas, *J. Phys. Chem. Solids* **49**, 213 (1988).
- ¹⁵A. Singh, V. Neu, S. Fähler, K. Nenkov, L. Schultz, and B. Holzapfel, *Phys. Rev. B* **77**, 104443 (2008).